JOURNAL OF CATALYSIS **113**, 529–534 (1988)

A Study of the Activity and Selectivity of Molybdenum Crystallographic Shear Compounds in the Oxidation of C_4 Hydrocarbons

Oxides which are catalysts in the selective oxidation of olefins are thought to form crystallographic shear (CS) structures (*1–3*). These structures can form as a result of the removal of lattice oxygen which leads to a change from corner to edge sharing of some of the metal–oxygen octahedra. Oxygen removal also results in reduction of some of the metal atoms to form a mixed valence solid (*4*). This work was undertaken with the goal of illuminating the role of these reduced molybdenum–oxygen structures in selective oxidation. In particular, several molybdenum CS compounds were studied and compared with MoO_3.

Molybdenum and tungsten CS compounds have been previously studied in olefin oxidation (*1, 5–8*). The role of CS in selective oxidation catalysis has also been the object of theoretical studies (*9*). It has been proposed that selective lattice oxygen insertion into the organic molecule occurs via shear structure formation (*2, 9*). In this mechanism one oxygen atom is evolved upon a change from corner to edge sharing of two metal–oxygen octahedra. In the experiments described here, several molybdenum CS compounds and MoO_3, which reduces by shear structure formation (*2, 9*), were studied in butene and butadiene oxidation. The CS compounds studied were $Mo_{18}O_{52}$ which contains shear planes within the layers of an MoO_3 substructure, Mo_8O_{23} in which the shear planes occur as ordered domains of edge sharing octahedra in an ReO_3 substructure, and two polymorphs of Mo_4O_{11} in which the shear planes are ordered domains of tetrahedrally coordinated Mo atoms in an ReO_3 substructure. The effects of oxide structure and of Mo oxidation state on selectivity were examined.

The CS compounds were synthesized by solid state reaction of stoichiometric mixtures of MoO_3 and MoO_2 in sealed, evacuated quartz tubes as described by Kihlborg and Mangelí (*10–14*) who also describe the structures of these compounds. Repeated homogenization was required to achieve complete reaction. The MoO_3 used was Fisher molybdic anhydride and the MoO_2 was acquired from Alpha Products. The products of the synthesis were identified by X-ray powder diffraction and the powder patterns were in close agreement with those reported in the literature (*15, 16*). A Siemans SRS 200 diffractometer and Cu$K\alpha$ radiation were employed. Laser Raman spectroscopy was used to detect the presence of MoO_3. BET surface areas were measured using a Micromeritics 2100E Accusorb volumetric surface analyzer with krypton as the adsorbate. The surface areas of the molybdenum oxides are listed in Table 1. X-ray photoelectron (XPS) spectra were obtained on an AEI 200B instrument using Al$K\alpha$ radiation. All spectra were referenced to a carbon 1*s* binding energy of 284.0 eV.

The maximum binding energies and full widths at half-maximum observed by XPS are listed in Table 2. Each spectrum was analyzed using a curve-fitting program called APES (analyzed photoelectron spectrum). APES smooths the data, adjusts the baseline, corrects for inelastic scattering, and fits a user-controlled number of components to the corrected spectrum using the method of nonlinear least squares. In per-

0021-9517/88 $3.00

TABLE 1

BET Surface Areas of the Molybdenum Oxides

Compound	Surface area (m^2/g)
MoO_3	0.40
$Mo_{18}O_{52}$	0.34
Mo_8O_{23}	0.21
Mo_4O_{11}-mon	0.16
Mo_4O_{11}-orh	0.42

forming this analysis, the presence of discrete, paramagnetic Mo^{5+} ions was ruled out because of the very low, positive values of magnetic susceptibility observed for all of these compounds (*17*). This assumption is supported by their lack of ESR signals over a wide range of temperature (*18*). Consequently, the user-specified components chosen in the curve-fitting analysis were Mo^{6+} and Mo^{4+} or broadened components. Component peak broadening may be thought of as being caused by electron delocalization which occurs in metal–ligand–metal or mixed valence electronic interactions (*19*).

Results of the curve-fitting analysis are also listed in Table 2. The spectrum of $Mo_{18}O_{52}$ was fit to one broad component suggesting near electronic equivalence of the Mo atoms. This idea is supported by the decreased spin–orbit splitting, relative to MoO_3, which indicates a higher degree of electron delocalization (*19*). It seems possible that the Mo atoms interact through Mo–O–Mo bonds at the shear planes where the structure is most condensed because of increased edge sharing between Mo/O octahedra relative to MoO_3. The XPS spectra of the Mo_4O_{11} polymorphs exhibit low binding energy shoulders and were fit with two slightly broadened components. The Mo^{6+}/Mo^{4+} ratios from this analysis lead to calculated average Mo oxidation states very close to 5.50. This value is the same as that calculated from stoichiometry and suggests that in the Mo_4O_{11} polymorphs the valences are trapped or localized. The analysis indicates that one-fourth of the Mo atoms are present as Mo^{4+}. The decreased level of condensation or edge sharing relative to MoO_3 in ReO_3-type structures may be responsible for the observed valence trapping.

The XPS spectrum of Mo_8O_{23} could not be fit under the assumptions employed here, possibly because of the presence of Mo^{5+} or Mo^{3+} ions as reported by others (*20*). However, these ions were not observed in ESR studies performed in our laboratory (*18*). The Mo_8O_{23} structure exhibits less edge sharing than that of $Mo_{18}O_{52}$ but more than that in Mo_4O_{11} and so a situation intermediate between valence delocalization and valence trapping might be expected. The increased spin–orbit splitting relative to MoO_3 may also indicate that some of the valences are trapped while peak broadening appears to indicate some degree of electron delocalization. The XPS spectrum of a solid in which some of the

TABLE 2

Maximum Binding Energies, Full Widths at Half-Maximum (eV) and Curve Fitting Results for Mo Oxide Photoelectron Spectra

Compound	O 1*s*	Mo 3$d_{5/2}$	Mo 3$d_{3/2}$	Mo^{6+}/Mo^{4+}
MoO_3	530.0 (1.84)	232.7 (1.59)	235.8 (1.49)	—
$Mo_{18}O_{52}$	529.8 (2.20)	232.4 (2.55)	235.3 (2.38)	Single comp.
Mo_8O_{23}	529.8 (2.13)	232.1 (2.56)	235.3 (2.46)	No fit
Mo_4O_{11}-mon	530.1 (3.31)	232.4 (2.65)	235.3 (2.39)	3.5
Mo_4O_{11}-orh	529.7 (2.46)	232.1 (2.35)	235.0 (2.05)	3.2

valences are trapped while others interact would be difficult to analyze using the curve-fitting method employed here.

The selectivity for butene and butadiene oxidation was studied in a $\frac{1}{4}$-in.-diameter by $1\frac{1}{2}$-in.-long, fixed bed reactor at 500°C. In preliminary, steady-state experiments using Mo_4O_{11}-orh and Mo_8O_{23} to oxidize 1-butene in air, nearly complete oxidation of the initially reduced catalyst occurred. The presence of MoO_3 in the postreaction samples was indicated by both Raman spectra and X-ray diffraction (*21*). Rapid oxidation of Mo_8O_{23} to MoO_3 in a steady-state reactor at 500°C has been observed before in studies of propylene oxidation (*8*). To avoid complete oxidation of the reduced oxides and to observe intermediate reaction products, experiments were performed in pulsed reactor mode. In order to compare the activity of the various compounds, the reactor was always loaded with the same surface area of catalyst (0.10 ± 0.01 m^2). The pulsed reaction experiment was performed with helium as the carrier gas flowing at a rate of 30 ml/min as metered by a Tylon Model FC 260 mass flow controller. Impurities in the helium were removed by passing over a Cu catalyst and a silica gel trap. A pulse of 0.5% hydrocarbon in air was introduced first. After the products were analyzed, this was followed by a second pulse of 0.5% hydrocarbon in N_2. This pulse sequence was performed three times for each catalyst using a fresh sample and analyzing for different products in each experiment by gas chromatography. Experimental details are described elsewhere (*21*).

The overall conversion of butene or butadiene and the selectivities to CO_2, butadiene (from butene), furan, and maleic anhydride are shown in Fig. 1 for each pulse. Nearly every experiment was repeated and the selectivities for these replications were within ±4%. As an overall check on the 1-butene reaction data, both empty reactor and SiC-packed reactor runs were made at 500°C in air. The products observed were trace amounts of CO_2 along with cracking and isomerization products. Conversions were less than 5%. No blank runs were made with butadiene as the feed.

When butene was the reactant, CO_2 formed only in the presence of O_2 and the selectivity to this undesirable product was highest over Mo_4O_{11}-orh at nearly 70%. All other phases produced significantly less CO_2 from butene with selectivities around 50%. The data for CO_2 formation from butadiene are different. In this case, the Mo_4O_{11} polymorphs produce more CO_2 than Mo_8O_{23} or $Mo_{18}O_{52}$, but approximately the same amount as MoO_3. Interestingly, Mo_4O_{11}-orh produces a small amount of CO_2 from butadiene even in the absence of gas-phase oxygen. The results suggest that oxygen activation for complete oxidation may be favored over surfaces containing trapped valences.

As can be seen in Figs. 1a and 1b, the oxidative dehydrogenation activity for converting butene to butadiene was not sensitive to oxide structure or to average oxidation state. The only difference observed in these experiments is that the selectivity to butadiene was 46% in the presence of O_2 and only 5% in the absence of O_2. Other studies have shown that molecular oxygen does not participate in the rate-limiting step of this reaction (*1*, *22*).

By far the most interesting data are those for the products of oxygen insertion. In butene oxidation, oxygen-containing organic compounds were formed only in the presence of O_2. In butadiene oxidation, however, oxygen insertion products were observed even in the absence of O_2. The data for maleic anhydride formation indicate a dependence on Mo oxidation state. Maleic anhydride formation from butene increased with degree of oxidation being highest for MoO_3 at nearly 50%. In butadiene oxidation, MoO_3 also produced the most maleic anhydride and produced maleic anhydride in the absence of molecular

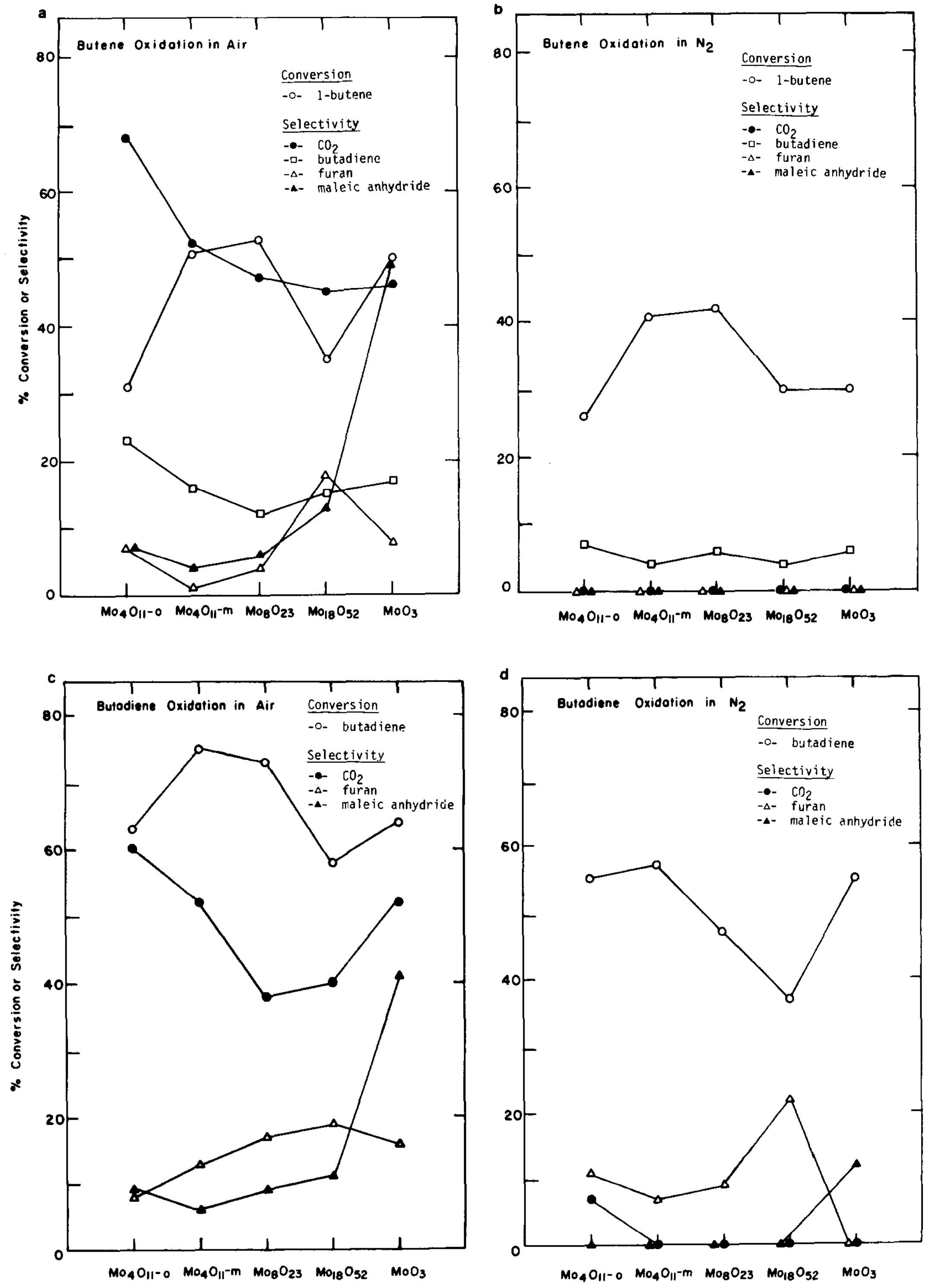

FIG. 1. Conversion and selectivity for (a) butene oxidation in air, (b) butene oxidation in N_2, (c) butadiene oxidation in air, and (d) butadiene oxidation in N_2.

oxygen. The formation of furan was observed from both butene and butadiene in the presence of O_2 and from butadiene in the absence of O_2. Significantly, more furan was formed from butadiene than from butene with a trend toward higher selectivities over more oxidized phases; however, $Mo_{18}O_{52}$, a reduced phase, produced the most furan. Furan formation was unaffected by the absence of oxygen over this solid. It is possible that $Mo_{18}O_{52}$ may contain surface sites that insert oxygen into butene and butadiene to form the furan ring structure. This catalyst has the MoO_3 basic structure and XPS results suggest that butene or butadiene adsorption as a furan precursor is favored over a slightly reduced surface where there is some electron mobility between surface atoms. This situation apparently occurs when CS structures form in an MoO_3 layer as in $Mo_{18}O_{52}$.

An explanation of these results is suggested by the work of Volta and co-workers (*23*). They have observed the formation of MoO_3 crystallites with unusual crystal face development on the surface of $Mo_{18}O_{52}$ under catalytic conditions. The crystallites had highly developed (100) and (101) or $(10\bar{1})$ faces and produced an increased selectivity to acrolein in propylene oxidation. Similar arguments can be used to explain the results presented here. For example, MoO_3 exhibited relatively high selectivities for both complete oxidation and selective oxygen insertion. $Mo_{18}O_{52}$ exhibits decreased CO_2 formation and a high oxygen insertion activity and may do so because the surface reconstructs or oxidizes to present specific MoO_3 crystal faces. The higher level of CO_2 formation observed over the more reduced phases such as Mo_4O_{11} may be accounted for by surface reconstruction to expose MoO_3 crystal faces specific for oxygen activation and complete oxidation to CO_2. The oxidative dehydrogenation of butene to form butadiene is apparently not sensitive to surface structure and is unaffected by MoO_3 crystal face development. Raman spectra acquired after the pulsed reaction studies were performed indicated the presence of MoO_3 in all samples; however, no studies yielding information on crystal face development were conducted.

In summary, the unusual coordination geometries and surface structures that are thought to be caused by the presence of CS planes in molybdenum oxides produce significant and interesting differences in the selectivities observed in oxidation catalysis. In particular, the high selectivity to furan observed over $Mo_{18}O_{52}$ indicates that some structural feature of this compound is important in the formation of furan without further oxidation to maleic anhydride. The structure of this compound may also enhance the formation of MoO_3 domains possessing surfaces specific to this reaction. Maleic anhydride formation was favored over the completely oxidized surface of MoO_3.

ACKNOWLEDGMENTS

This work was conducted through the Ames Laboratory which is operated for the U.S. Department of Energy by Iowa State University under Contract W-7405-ENG-82. This work was supported by the Office of Basic Energy Sciences.

REFERENCES

1. Batist, Ph. A., Kapteyns, C. J., Lippens, B. C., and Schuit, G. C. A., *J. Catal.* **7,** 33 (1967).
2. Haber, J., Marczewski, W., Stoch, J., and Ungier, L., *Ber. Bunsen. Ges. Phys. Chem.* **79**(11), 970 (1975).
3. Serwicka, E., *J. Solid State Chem.* **51,** 300 (1984).
4. Robin, M. B., and Day, P., *Adv. Inorg. Chem. Radiochem.* **10,** 247 (1967).
5. Barber, S., Booth, J., Pyke, D. R., Reid, R., and Tilley, R. J. D., *J. Catal.* **77,** 180 (1982).
6. DeRossi, S., Iguchi, E., Schiavello, M., and Tilley, R. J. D., *Z. Phys. Chem.* **103,** 193 (1976).
7. DeRossi, S., Iguchi, E., Schiavello, M., and Tilley, R. J. D., *J. Catal.* **61,** 256 (1980).
8. Haber, J., Janas, J., Schiavello, M., and Tilley, R. J. D., *J. Catal.* **82,** 395 (1983).
9. Broclawik, E., and Haber, J., *J. Catal.* **72,** 379 (1981).
10. Kihlborg, L., *Ark. Kemi* **21**(44), 471 (1963).
11. Kihlborg, L., *Ark. Kemi* **21**(34), 357 (1963).
12. Kihlborg, L., *Ark. Kemi* **21**(42), 443 (1963).

13. Magnelí, A., *Acta Chem. Scand.* **2,** 501 (1948).
14. Kihlborg, L., *Ark. Kemi* **21**(35), 365 (1963).
15. Kihlborg, L., *Acta Chem. Scand.* **13,** 954 (1959).
16. Magnelí, A., Andersson, G., Blomberg, B., and Kihlborg, L., *Anal. Chem.* **24**(12), 1998 (1952).
17. Gruber, H., Haselmair, H., and Fritzer, H. P., *J. Solid State Chem.* **47,** 84 (1983).
18. McCormick, R. L., and Schrader, G. L., unpublished results.
19. Baker, A. D., and Brundle, C. R., "Electron Spectroscopy," Vol. 1. Academic Press, New York, 1977.
20. Hedewy, S., and Abu-El Saud, A., *Acta Phys. Pol. A* **67,** 1085 (1985).
21. McCormick, R. L., M. S. thesis, Iowa State University, 1984.
22. Batist, Ph.A., Der Kinderen, A. H. W. M., Leeuwenburgh, Y., Metz, F. A. M. G., and Schuit, G. C. A., *J. Catal.* **12,** 45 (1968).
23. Volta, J.-C., Bertrand, O., and Floquet, N., *Chem. Commun.*, 1283 (1985).

ROBERT L. MCCORMICK[1]
G. L. SCHRADER

Department of Chemical Engineering
Iowa State University
Ames, Iowa 50010
Ames Laboratory
U.S. Department of Energy
Ames, Iowa 50011

Received June 1, 1987; revised March 29, 1988

---

[1] To whom correspondence should be addressed at AMAX Research and Development Center, Golden, CO 80403.